CHAPTER 14

TRANSFORMATION OF WAVE CREST PATTERN IN SHOALING WATER

Yoshimi Goda[1]

Abstract

Spatial distributions of wave crests are examined through numerical simulations of directional random sea surface. As the directional spreading of wave energy becomes narrow, the wave crests become long and the spread of individual crest directions become narrow. Simulations are extended to waves propagating into a planar beach. The areas of wave breaking are identified as the zone of surface elevation higher than the breaking threshold. The lateral spreading speed of breakers is analyzed from consecutive scenes of breaker crest patterns. It is about 30% of the forward advance speed of breakers.

Introduction

Directional random sea waves are generally described with the directional wave spectrum. The wave field is represented as the superposition of an infinite number of infinitesimal component waves, as illustrated by Pierson, Neumann, and James (1955). The theoretical expression for the root-mean-square wave number in an arbitrary direction has been given by Longuet-Higgins (1957), who introduced the long-crestedness parameter as the ratio of the smallest to the largest wave numbers in the directions 90° degree apart. Isobe (1988) introduced a theory of the joint distribution for the direction, height, and period of individual waves, based on the orbital velocities of water particles on the surface. Such statistics on individual wave directions are the subject to be examined in more details in the present paper.

A direct approach to the statistics of individual wave directions is to analyze the spatial distributions of sea surface elevations. The data of real sea surface elevations are hard to obtain, but the simulation technique can provide as many data as necessary. The contours of simulated wave surface make it possible to identify the areas of wave crests, on which the lengths, heights, and directions of wave crests are examined. The information on the statistics of wave crests will be utilized for the analysis of surfing climate, the necessity of which has been pointed out by Dally (1990).

---

[1] Prof., Yokohama National Univ., Dept. Civil Eng., Hodogaya-Ku, Yokohama 240, Japan, M. ASCE

Analysis of wave crest statistics has been undertaken by Goda and Tokiwa (1991) and by Goda and Mizusawa (1992), but the results are reported in Japanese. The present paper introduces the directional characteristics of wave crests in both uniform and shoaling waters. The aspect of crest length statistics will be reported elsewhere (Goda 1993).

Directional Wave Spectrum Employed for Simulation

A combination of the modified JONSWAP frequency spectrum and the Mitsuyasu-type directional spreading function was employed as the directional spectrum for numerical simulations. For a given wave height $H_{1/3}$ and spectral peak period T_p , the modified JONSWAP spectrum is expressed by Goda (1988) as

$$S(f) = \beta_J H_{1/3}^2 T_p^{-4} f^{-5} \exp[-1.25(T_p f)^{-4}] \, \gamma^{\exp[-(T_p f - 1)^2/\sigma^2]} \qquad (1)$$

where

$$\beta_J = \frac{0.0624[1.094 - 0.01915 \ln \gamma]}{0.230 + 0.0336\gamma - 0.185(1 + \gamma)^{-1}} \qquad (2)$$

$$\sigma = \begin{cases} 0.07 & : f \le f_p \\ 0.09 & : f > f_p \end{cases} \qquad (3)$$

Throughout the simulations, the following height, period, and peak enhancement factor were employed:

$$(H_{1/3})_0 = 2.0 \, \text{m}, \qquad (T_p)_0 = 8.01 \, \text{s}, \qquad \gamma = 3.3 \qquad (4)$$

where the subscript 0 indicates the values of deepwater waves. The spectral peak period of 8.01 s corresponds to the deepwater wave length of $(L_p)_0 = 100.0$ m. The significant wave period is estimated as $T_{1/3} = 7.59$ s. Because the wave linearity is assumed and the results are all presented in dimensionless forms, the above values of height and period merely indicate the input conditions for simulations.

The Mitsuyasu-type directional spreading function is expressed as

$$G(f; \theta) = G_0 \cos^{2S}(\theta/2) \qquad (5)$$

where

$$G_0 = \left[\int_{\theta_{\min}}^{\theta_{\max}} \cos^{2S}(\theta/2) d\theta \right]^{-1} \qquad (6)$$

$$S = \begin{cases} (f/f_p)^5 \, S_{\max} & : f \le f_p \\ (f/f_p)^{-2.5} \, S_{\max} & : f > f_p \end{cases} \qquad (7)$$

The directional spreading parameter $S_{\max}$ was given the values of $10, 25$, and 75 to represent wind waves, medium-distance swell, and long-distance swell.

Simulations of Directional Random Wave Profiles in Water of Uniform Depth

The surface elevation of directional random waves $\eta(x, y)$ is computed by means of double series of the following form:

$$\eta(x, y) = \sum_{m=1}^{M} \sum_{n=1}^{N} a_{m,n} \cos(k_m x \cos \alpha_n + k_m y \sin \alpha_n + \epsilon_{m,n}) \qquad (8)$$

where $a_{m,n}$ denotes the amplitude of component wave, k_m the wave number, α_n the directional angle, x and y the cartesian coordinates, and $\epsilon_{m,n}$ the random phase angle which is uniformly distributed between 0 and 2π. The time t is dropped in Eq. 8, because the wave profiles in steady state condition is examined in the water of uniform depth.

The number of frequency components was set at $M = 50$, while that of directional components was $N = 30$. The wave number k_m was computed by the small amplitude wave theory for the following frequency f_m :

$$f_m = 1.007 \, T_{1/3}^{-1} \, \{\ln[2M/(2m-1)]\}^{-1/4} \tag{9}$$

The directional angle α_n was set by equally dividing the directional range between $[(\alpha_p)_0 - 90°]$ and $+90°$ in deepwater, where $(\alpha_p)_0$ denotes the incident wave angle to the depth contour in deepwater. In shallow water, the directional range was reduced by considering the wave refraction effect.

Wave simulations were carried out in deepwater and also in shallow water with the depth $h = 20, 10$, and 5 m, which corresponded to the relative water depth $h/L_0 = 0.2, 0.1$, and 0.05, respectively. The shoaling and refraction effects were taken into account in wave simulations in shallow water, by assuming the depth contours being parallel and straight lines. The bottom slope was assumed nearly horizontal so that the area of computation could be considered of the uniform depth.

The computation area was a square with the side length equal to $20(L_p)_0$, and the grid spacing of $\Delta x = \Delta y = 0.1(L_p)_0$ was employed. For a given condition of wave simulation, 25 surface wave profiles were created by changing the initial phase angle by means of a pseudo random number generating program.
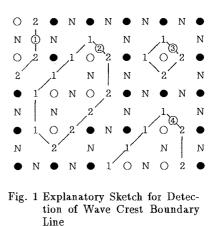
Detection and Definition of Wave Crests

Wave crests can be defined in many ways. In this paper a wave crest is defined as an enclosed area above a certain threshold elevation. The outermost boundary of this wave crest area defines the length, width, direction of the wave crest. The procedure to detect and define the outermost boundary is as follows.

First, the surface elevation at every grid point in the computed space is cheked if it is above the threshold level, and the grid point is marked accordingly. The closed circles in Fig. 1 indicate the point being below the threshold level, while the open circles being equal to or above the threshold level.

Second, a search is made for a change from the open to closed circles or vice versa between the adjoining grid points. The search is made from the left to the right and from the top to the bottom along every grid line. When the change from a closed circle to an open circle takes place, the numeral 1 is assigned to the section of grid line there. The change from an open circle to a closed circle is marked with the numeral 2. No change is marked with N.

Third, a line is drawn by connecting the sections of grid lines marked either with 1 or 2. When such lines are drawn, they are numbered as ①, ②, ③, and so on. These lines are examined if they encounter the peripheries of the computation area. When a line does not form a closed loop by ending up at the peripheries, it is not considered as a complete boundary of wave crest and discarded in the following analysis.

Fourth, the exact location of the wave crest line is determined at each grid line section by a linear interpolation between the surface elevations at the adjoining grid points. The information of the locations of grid-line-crossings is stored for each wave crest line for further analysis.

The threshold elevation for defining wave crests was selected as $\eta_{\text{thres.}} = 0.1(H_{1/3})_0$ after several examinations. This threshold level is employed throughout this paper except for the case when the breaker area is defined.

Fig. 1 Explanatory Sketch for Detection of Wave Crest Boundary Line

Wave Crest Patterns and Crest Lengths in Water of Uniform Depth

Figure 2 exhibits examples of wave crest areas defined by the above procedure. The four diagrams shown here represent directional random waves with the spreading parameter $(S_{\max})_0 = 25$ in water of uniform depth. The upper left diagram is for deepwater waves, and the other three diagrams are for waves with the relative depth $h/L_0 = 0.2, 0.1$, and 0.05. The incident wave angle is $(\alpha_p)_0 = 30°$. As the relative depth decreases, wave crest patterns approach toward the pattern of monocromatic waves, because of the wave refraction and shoaling effects. The apparent long-crestedness of wave patterns in shallow water regions is caused by the shortening in wave length: the absolute lengths of wave crests remain unchanged from deep to shallow water for the same value of directional spreading parameter.

The directional spreading affects the wave crest length. As the range of directional spreading becomes narrow, the crest length increases. Figure 3 shows the relation between the relative crest length λ/L_p and the directional spreading parameter $S_{\max}^*$. The crest lengths are measured for crests with the top elevation η_c higher than $0.75(H_{1/3})_0$, and the mean length and the upper quartile length have been calculated from the data of 25 wave crest patterns for each condition. The crest lengths are normalized with the local wave length L_p corresponding to the spectral peak frequency. For waves in the intermediate to shallow water, the directional spreading becomes narrow owing to the wave refraction effect. This causes an apparent increase in the value of $S_{\max}$ as shown in Fig. 4 (Goda and Suzuki 1975), which is called the equivalent spreading parameter in this paper. The closed symbols in Fig. 3 refer to waves with $(S_{\max})_0 = 25$ in the intermediate to shallow water. As shown in Fig. 3, the relative crest length is well described as the function of equivalent spreading parameter $S_{\max}^*$ regardless of water depth.

Spreading of Individual Crest Directions

The crest direction is defined as the direction normal to the straight line connecting the two outermost points of a wave crest area. Figure 5 shows the joint distribution of the crest direction θ and the relative crest length $\lambda/(L_p)_0$ of the random waves with $S_{\max} = 10$ in deep water, while Fig. 6 is for waves with $(S_{\max})_0 = 25$ in shallow water with $h/L_0 = 0.05$. The numerals in Figs. 5 and
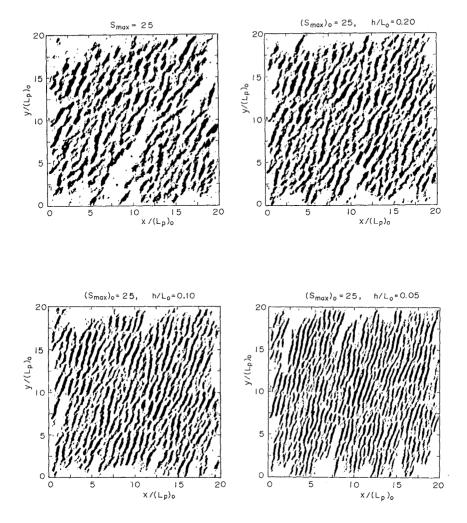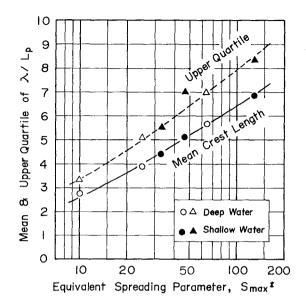
Fig. 2 Wave Crest Patterns in Water of Uniform Depth

Fig. 3   Mean and Quartile Crest Lengths of Wave Crests Higher
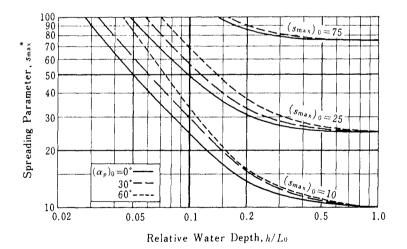   than $0.75(H_{1/3})_0$

Fig. 4   Equivalent Spreading Parameter S_{max}^* in Shallow Water
          Area (after Goda and Suzuki 1975)

6 are the numbers of wave crests within respective blocks of relative crest length and crest direction. The data with crest lengths less than $(L_p)_0$ are omitted because of inherent errors in assessing the crest direction (the positions of wave crest lines are determined on the x and y grid lines only).

The incident wave angle in deep water is $(\alpha_p)_0 = 30°$. The mean angle of crest direction in Fig. 5 is 27.8°, and a small difference is probably due to the method of defining crest direction. The mean angle of crest direction in Fig. 6 is 13.0°, which is slightly smaller than the mean direction 15.0° estimated by the calculation of wave refraction with the directional spectrum.
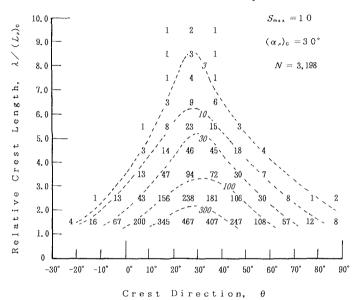

Fig. 5   Joint Distribution of Individual Crest Direction and Relative
          Crest Length in Deepwater with $S_{\max} = 10$

The spread of individual crest directions is represented with their standard deviations. They are plotted against the equivalent spreading parameter $S_{\max}{}^*$ in Fig. 7, where the standard deviation of crest direction for the wave crests longer than $(L_p)_0$ and that of crests higher than $0.75(H_{1/3})_0$ are shown.

Simulation of Directional Random Wave Patterns in Shoaling Water

Waves propagating in shoaling water can be simulated by paying due account to the change in phase angle. For the case of one-dimensional waves, the phase angle advances by the amount $k\,dx$ over a distance dx. When waves propagate from x_0 to x_I and reach to the I-th grid section, the wave profiles there can be computed by using the following equation:

$$\eta(x_I, t) = a(x_I) \cos[2\pi f t + \epsilon + \sum_{i=0}^{I-1} k(x_i)dx] \tag{10}$$
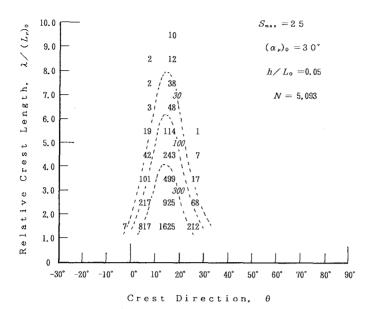
Fig. 6   Joint Distribution of Individual Crest Direction and Relative Crest Length in Shallow Water at $h/L_0 = 0.05$ with $(S_{\max})_0 = 25$
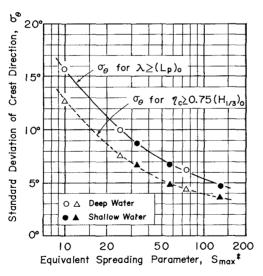

Fig. 7   Standard Deviation of Individual Crest Directions of Wave Crests Longer than $(L_p)_0$ and Those of Crest Lengths Higher than $0.75(H_{1/3})_0$

in which i denotes the order number of the grid section and ϵ is the initial phase angle. The amplitude a is a function of the location x_I due to the shoaling effect.

Waves propagating toward the shore of coast with parallel straight contours are depicted in Fig. 8. The coordinate x is set parallel to the shoreline and thus the water depth is constant in the y direction. The lines with arrows indicate the direction of wave propagation and the dashed lines normal to the arrow lines represent the wave crest lines. The phase angle at each grid point is determined as follows. First, the phase angle at (x_0, y_1) is greater by the amount $k(x_0)dy\sin\alpha(x_0)$ than that at the origin (x_0, y_0). The advance of phase angle at (x_0, y_J) is J times that amount. Along the line $y = y_J$ the phase angle increases by the amount $k(x_i)\cos\alpha(x_i)$ when waves propagate from the i-th section to $(i+1)$-th section. This increase of phase angle is common for all the y-lines. Thus, the wave profile at the grid section (x_I, y_J) can be calculated by the following equation:
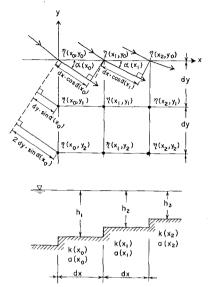

Fig. 8   Explanatory Sketch for Grid System of Planar Beach

$$\eta(x_I, y_J) = a(x_I)\cos\Big[-2\pi ft + \epsilon + k(x_0)Jdy\sin\alpha(x_0)$$
$$+ \sum_{i=0}^{I-1} k(x_i)dx\cos\alpha(x_i)\Big] \tag{11}$$

Wave simulation in shoaling water has been carried out by using Eq. 11, and wave crest areas have been marked out as exemplified in Fig. 9. The bottom slope is assumed as 1/100, and the wave crest pattern in the water depth from 20 m to 0.1 m are shown there. The incident wave conditions are the same as those in Fig.2.

Spatial Behavior of Breaking Waves in the Surf Zone

The area in which waves are breaking can be detected through examination of the spatial surface elevations of random waves. It is done by setting the threshold level of wave crest definition at some breaking crest elevation instead of a fixed value such as $\eta_{\text{thres.}} = 0.1(H_{1/3})_0$. The threshold level of breaking crest area is set in this paper as one-half the breaker height formulated by Goda (1975), i.e.:

$$\eta_b = \frac{1}{2}H_b = 0.085L_0\left\{1 - \exp\left[-1.5\frac{\pi h}{L_0}(1 + 15\tan^{4/3}\theta)\right]\right\} \tag{12}$$

where $\tan\theta$ denotes the bottom slope. The threshold level varies with the x coordinate, but the technique of defining the breaking crest area is the same as before. However, the crest lines crossing the peripheries of the simulation area have been kept as the boundary of breaking area.
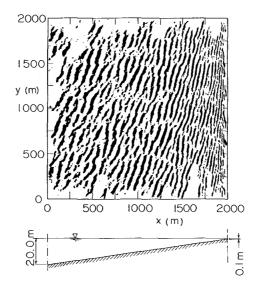
Fig. 9   Wave Crest Pattern in Shoaling Water of Planar Beach with
          $(S_{max})_0 = 25$ and $(\alpha_p)_0 = 30°$

A check on the reliability of simulating random surface elevations has been
made by comparing the ratio of breaking wave crest areas to the total water area
in a given water depth. From the simulated surface elevations, the total length
of breaking wave crests along a given grid line at a constant x-value (constant
water depth) was tabulated and this process was repeated at each grid line. The
total length of breaking crest areas when divided by the length $20(L_p)_0$ provides
the breaker ratio at a given water depth. The raw data of breaker ratio has been
averaged over 25 diagrams of random wave profiles in order to reduce the effect
of statistical variability. The dashed line in Fig. 10 is a result of such analysis.

The theoretical prediction of breaker ratio has been made through the com-
putation of shoaling and refraction of directional random waves. The root-mean-
square value of deepwater waves has been transformed to that of shallow water
waves by being multiplied with the shoaling and refraction coefficients of di-
rectional spectral waves. Because the wave simulation is based on the linear
superposition of component waves, the simulated wave elevations should follow
the normal distribution. Then the probability of surface elevation exceeding the
breaker threshold level by Eq. 12 is simply estimated from the probability table
of the normal distribution. The predicted value is shown with the solid line in
Fig. 10, and it fits with the result of simulation analysis as expected.

The effect of incident angle upon the breaker ratio is demonstrated in Fig.
11. As the incident angle increases, the breaker ratio at a given depth decreases
slightly; the start of wave breaking becomes closer to the shoreline and the surf
zone becomes a little narrow. This is due to the more conspicuous decrease in
the local wave height by the wave refraction effect in the case of oblique wave
incidence than that of the normal wave incidence. The difference between the
breaker ratios of different incident angles have also been predicted by theoretical

$(S_{max})_0 = 25$, $(H_{1/3})_0 = 2.0$ m

$(\alpha_p)_0 = 30°$

Theory ———
Simulation -----

Breaker Ratio, P (%)

Water Depth, h (m)

$(S_{max})_0 = 25$, $(H_{1/3})_0 = 2.0$ m

$(\alpha_p)_0 = 0°$ ------
$30°$ -----
$60°$ ---·--
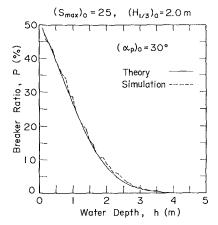
Breaker Ratio, P (%)

Water Depth, h (m)

Fig. 10 Comparison of Theoretical and Simulated Ratios of Breaker Areas
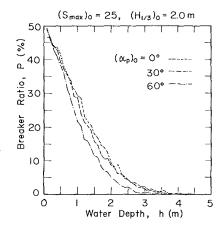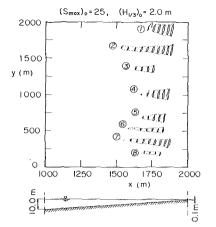
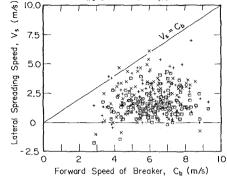Fig. 11 Effect of Incident Wave Angle on Breaker Ratio

calculation, though not shown in Fig. 11.

Growth of Wave Breaking Areas in Shoaling Water

Wave simulations can also reveal the change of individual breaking crest areas. Figure 12 exhibits an example of such analysis. A simulation of wave profiles in the nearshore is made with a certain set of initial phase angles. Then the transformation of that wave profiles is followed from $t = 0$ to $t = 9T_p$ with the time step $\Delta t = T_p$ by using the same set of initial phase angles and by changing the time t in Eq. 11. Among these consecutive scenes of wave profiles, visual search is made for conspicuous breaking areas which appear in the locations far from the shoreline. Once they are picked up, further search is carried out on the locations of the same breaking areas in the preceding and following scenes. The breaking crest area marked with ② in Fig. 12, for example, has been noted in all of ten simulated wave profiles and its growth has been well observed, whereas the rest of breaking crest areas have appeared at later scenes. In the analysis of the time-sequence change of breaking crest areas, the grid distance $\Delta x = 5$ m was adopted for finer resolution. The number of grid lines and the bottom slope were the same as before so that the offshoreward water depth was 10.0 m.

The shoreward advances of conspicuous breaking crest areas have been plotted on tracing papers, and the lateral spread lengths of these crest area have been measured on the tracing papers. The lateral spreading speed V_s of the breaking crest area has been calculated from these data. Figure 13 shows the results of the analysis of the lateral spreading speed of breaking crest area. The abscissa is the forward advance speed C_b of breaker, which has been approximated as $\sqrt{gh}$ with the water depth h at the corresponding locations. The analysis has been carried out for the deepwater directional spreading parameter of $(S_{max})_0 = 10, 25$, and 75, but the effect of directional spreading parameter on the lateral spreading speed is insignificant. As seen in Fig. 13, the lateral spreading speed shows a large scatter, but it remains in the range between 0 and C_b. The regression line

$(S_{max})_0 = 25$, $(H_{1/3})_0 = 2.0$ m

$(H_{1/3})_0 = 2.0$ m, $(\alpha_p)_0 = 30°$

Fig. 12 Time Sequence Change of Breaker Areas with Time Step $\Delta t = T_p$

Fig. 13 Lateral Spreading Speed versus Forward Speed of Breaking Crests [□: $(S_{max})_0 = 10$, +: $(S_{max})_0 = 25$, ×: $(S_{max})_0 = 75$]

between V_s and C_b under the condition that the line should pass through the origin yields the relation $V_s = 0.30C_b$.

Conclusions

Numerical simulation of directional random sea surface has succeeded in visualizing the wave crest patterns and clarifying the statistics of wave crest lengths and directions. Major conclusions of the present paper can be summarized as follows:

1. The mean crest lengths and the standard deviation of crest directions are governed by the directional spreading parameter S_{max} of the Mitsuyasu-type directional function.

2. In shoaling water, the effect of relative water depth on the crest statistics can be incorporated by using the equivalent spreading parameter S_{max}^* shown in Fig. 4.

3. The portion of breaking area within wave crests in shoaling water can be identified by setting the threshold surface level at the breaking crest elevation at respective water depth.

4. The lateral spreading speed of breaking crest area shows a wide scatter, but the average speed is assessed as 0.3 times the forward advance speed of breaker.

The numerical simulations reported hereinabove have been carried out by Messrs. Yasuhiro Tokiwa and Tatsuya Mizusawa as their thesis works at the Department of Civil Engineering, Yokohama National University. The author wishes to express his deep appreciation for their cooperations.

References

Dally, W. R. (1990): Stochastic modeling of surfing climate, *Proc. 22nd Int. Conf. Coastal Eng.*, pp.516-529.

Goda, Y. (1975): Irregular wave deformation in the surf zone, *Coastal Engineering in Japan*, Vol.18, pp.13-26.

Goda, Y. (1988): Statistical variability of sea state parameters as a function of wave spectrum, *Coastal Engineering in Japan*, Vol.31, No.1, pp.39-52.

Goda, Y. (1993): Statistics of wave crest lengths based on directional wave simulations, OMAE '93 (to be presented).

Goda, Y. and Mizusawa, T. (1992): Wave crest statistics based on numerical simulations: Longitudinal profiles and breaking characteristics, *Proc. Coastal Eng., JSCE*, Vol.39, pp.106-110 (*in Japanese*).

Goda, Y. and Suzuki, Y. (1975): Computation of refraction and diffraction of sea waves with Mitsuyasu's directional spectrum, *Tech. Note of Port and Harbour Res. Inst.*, No.230, 45p. (*in Japanese*).

Goda, Y. and Tokiwa, Y. (1991): Wave crest statistics based on numerical simulations, *Proc. Coastal Eng., JSCE*, Vol.38, pp.141-145 (*in Japanese*).

Isobe, M. (1988): On joint distribution of wave heights and directions, *Proc. Int. Conf. Coastal Eng.*, pp.524-538.

Longuet-Higgins, M.S. (1957): The statistical analysis of a random, moving surface, *Phil. Trans. Roy. Soc.*, Ser.A(966), Vol.249, pp.321-387.

Pierson, W. J., Jr., Neumann, G., and James, R. W. (1955): *Practical Methods for Observing and Forecasting Ocean Waves by Means of Wave Spectra and Statistics*, U. S. Navy Hydrogr. Office Pub. No. 603.